Adhesive lipophilic gels delivering rapamycin prevent oral leukoplakia from malignant transformation

Yuqi Du [a,b], Tiannan Liu [b], Tingting Ding [a], Xin Zeng [b], Qianming Chen [a], Hang Zhao [b,*]

[a] *Stomatology Hospital, School of Stomatology, Zhejiang University School of Medicine, Zhejiang Provincial Clinical Research Center for Oral Diseases, Key Laboratory of Oral Biomedical Research of Zhejiang Province, Cancer Center of Zhejiang University, Engineering Research Center of Oral Biomaterials and Devices of Zhejiang Province, Hangzhou, 310000, PR China*

[b] *State Key Laboratory of Oral Diseases, National Clinical Research Center for Oral Diseases, Chinese Academy of Medical Sciences Research Unit of Oral Carcinogenesis and Management, Med-X Center for Materials, West China Hospital of Stomatology, Sichuan University, Chengdu, Sichuan, 610041, PR China*

A B S T R A C T

Oral leukoplakia (OLK) is the most emblematic oral potentially malignant disorder that may precede the diagnosis of oral squamous cell carcinoma (OSCC) and has an overall malignant transformation rate of 9.8 %. Early intervention is crucial to reduce the malignant transformation rate from OLK to OSCC but the lack of effective local pharmaceutical preparations poses a challenge to clinical management. Rapamycin is speculated to prevent OLK from carcinogenesis and its inherent lipophilicity facilitates its penetration into stratum corneum. Nevertheless, hydrophilic hydrogels frequently encounter challenges when attempting to deliver lipophilic drugs. Furthermore, the oral cavity presents a complex environment defined by oral motor functions, saliva secretion cycles, dynamic fluctuations, and protective barriers comprising mucus and lipid layers. Consequently, addressing issues of muco-penetration and muco-adhesion is imperative for developing an effective drug delivery system aiming at delivering rapamycin to target oral potentially malignant disorders.

Here, a dual-function hydrogel drug delivery system integrating adhesion and lipophilicity was successfully developed based on polyvinyl alcohol (PVA) and dioleoyl phosphatidylglycerol (DOPG) via dynamic boronic ester bonds. Rheological experiments based on orthogonal design revealed that PVA-DOPG hydrogels exhibited ideal adhesive strength (around 6 kPa) and could adhere to various surfaces in both dry and wet conditions. PVA-DOPG hydrogels also significantly promoted lipophilic molecules' penetration into stratum corneum (integrated fluorescence density of $6.95 \pm 0.52 \times 10^6$ and mean fluorescence depth of 0.96 ± 0.07 mm) of ex-vivo porcine buccal mucosa ($p < 0.001$). Furthermore, PVA-DOPG hydrogels incorporating rapamycin inhibited malignant transformation of OLK mouse model induced by 4-Nitroquinoline N-oxide (4-NQO), distinct improvements in survival (the neoplasm incidence density at the 40th day is 0.0091) ($p < 0.05$), decrease in neoplasm incidence density of 36.36 % and inhibition rate in neoplasm volume of 75.04 ± 33.67 % have been demonstrated, suggesting the hydrogels were valuable candidates for potential applications in the management of OLK.

1. Introduction

Oral leukoplakia (OLK) is the most emblematic oral potentially malignant disorder that may precede the diagnosis of oral squamous cell carcinoma (OSCC) and has an overall malignant transformation rate of 9.8 % [1]. Early intervention is crucial to reduce the malignant transformation rate from OLK to OSCC and it is always an enduring topic among researchers and clinicians. Medications such as retinoids, carotenoids, and curcumin are employed in clinical settings to mitigate the malignant transformation rate of OLK; however, their efficacy remains uncertain, and side effects are frequently observed [2–4].

Components of the protein kinase B (AKT)/mammalian target of rapamycin (mTOR) pathway are intrinsic factors for carcinogenesis. The expression of mTOR protein is significantly elevated in OSCC and OLK, and the phosphorylation of mTOR protein increases with escalating dysplasia [5–7]. Tashiro et al. reported that phosphorylated mTOR (pmTOR) reactivity was significantly decreased in leukoplakia without epithelial dysplasia compared to that in mild to moderate dysplasia, moderate to severe dysplasia or carcinoma in situ ($p < 0.001$), and OSCC. A meta-analysis noted that mono-therapeutic mTOR inhibitors

resulted in stabilization of disease (52.5 %), but partial response (48.1 %) was reached when mTOR inhibitors were combined with chemotherapy and/or radiation. Rapamycin, renowned for its effectiveness as an inhibitor of mTOR protein and its reported ability to delay the progression of various cancers [8–10], which is speculated to prevent OLK from carcinogenesis. Unfortunately, its application is limited due to its inherent limited hydrophilicity, low oral bioavailability, obvious first-pass elimination effect and possible immunosuppression effect due to systemic application [11–13].

A local delivery system for rapamycin may take advantage of its inherent lipophilicity to enhance the penetration into the stratum corneum, thereby boosting local concentration and reducing the risk of immunosuppression. The barriers posed by the mucus and lipid layers in the oral cavity favor the passage and penetration of lipophilic molecules. Therefore, lipophilicity stands as a fundamental property to prioritize when seeking optimal solubility and uniform distribution. Furthermore, the oral cavity, being a moist and intricate environment, is characterized by a saliva-secreting cycle and oral motor functions [14,15]. Overcoming the challenges posed by moisture and motor functions contributes to achieving prolonged retention time. Therefore, adhesion emerges as another crucial factor that must be carefully considered [16–18].

Hydrogels, prized for their extended retention time, serve as valuable local drug carriers and find wide application in the topical treatment of various diseases. Polyvinyl alcohol (PVA) contains abundant hydroxy groups that can form hydrogen bonds and electrostatic interactions, contributing to the establishment of adhesive force [19–22]. PVA-based hydrogels have been utilized in various medical applications such as tissue engineering and wound dressing, where their adhesive properties are highly advantageous [23,24]. Pace et al. developed triboelectric nanogenerators based on amorphous PVA with high density of hydroxyl groups and amorphous structure present enabling a strong binding to water molecules and stronger adhesive contact [25]. Nonetheless, those hydrogels often contain excessive water content, making them unsuitable for carrying lipophilic medications. Incorporating lipids has been shown to enhance the lipophilicity of hydrogels and boost the solubility of lipophilic compounds. This, in turn, promotes the dispersion and diffusion of lipophilic molecules within the hydrogels [26–28]. Dioleoyl phosphatidylglycerol (DOPG) is a long-chain lipid with adjacent hydroxy groups at one end [29,30]. Additionally, borates can form boronic ester bonds with 1,2-diol or 1,3-diol groups, which not only strengthen the network structure but also endow hydrogels with responsiveness to environmental stimuli [31–33]. Our team has successfully developed a series of drug delivery systems based on boronic ester bonds [34–36].

Building upon the aforementioned points, it is hypothesized that lipophilic and adhesive hydrogels formulated using polyvinyl alcohol (PVA) and dioleoyl phosphatidylglycerol (DOPG) through boronic ester bonds could be developed and incorporating rapamycin into those PVA-DOPG hydrogels might potentially create an effective topical formulation for preventing carcinogenesis of OLK (Fig. 1).

2. Results

2.1. Construction and characterization of PVA-DOPG hydrogels

On one hand, the oral cavity is a humid and intricate environment characterized by a saliva-secreting cycle and oral motor functions. The hydrogels used are expected to be adhesive to ensure extended retention time. In this study, molecular weight of PVA, hydrolysis degrees of PVA, sodium borate, heating time and heating temperature have been chosen to design an orthogonal experiment (Appendix Table 1). Adhesive force was measured through rheological tests (Appendix Table 2) and analyzed with Minitab software (Fig. 2a). Results showed that the range of the five factors and their influence on the adhesive force above were as follows: molecular weight > hydrolysis degrees > heating temperature > sodium borate > heating time (Appendix Table 3) (Fig. 2b). Molecular weight and hydrolysis degrees significantly influenced the adhesive force of the hydrogels (Appendix Table 4). Consequently, in practical application, level 2 for molecular weight, hydrolysis degrees, and sodium borate were maintained, while level 2 for heating temperature and heating time were selected to ensure a more uniform
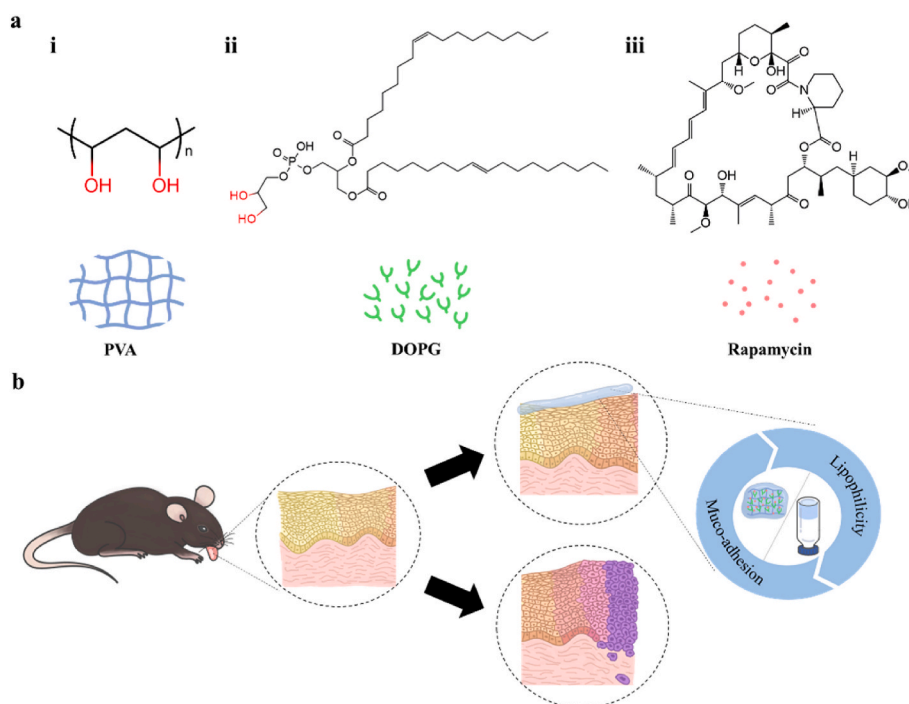
Fig. 1. Schematic summary of PVA-DOPG hydrogels loaded with rapamycin preventing malignant transformation of OLK: (a) Structural formula and diagrammatic drawing of PVA (i), DOPG (ii) and rapamycin (iii). (b) In mouse models exposed to a constant supply of 4-Nitroquinoline 1-oxide (4-NQO) in drinking water, lipophilic and adhesive hydrogels containing rapamycin are applied to prevent malignant transformation of oral epithelial cells. Conversely, the untreated group shows a significant occurrence of malignant transformation.
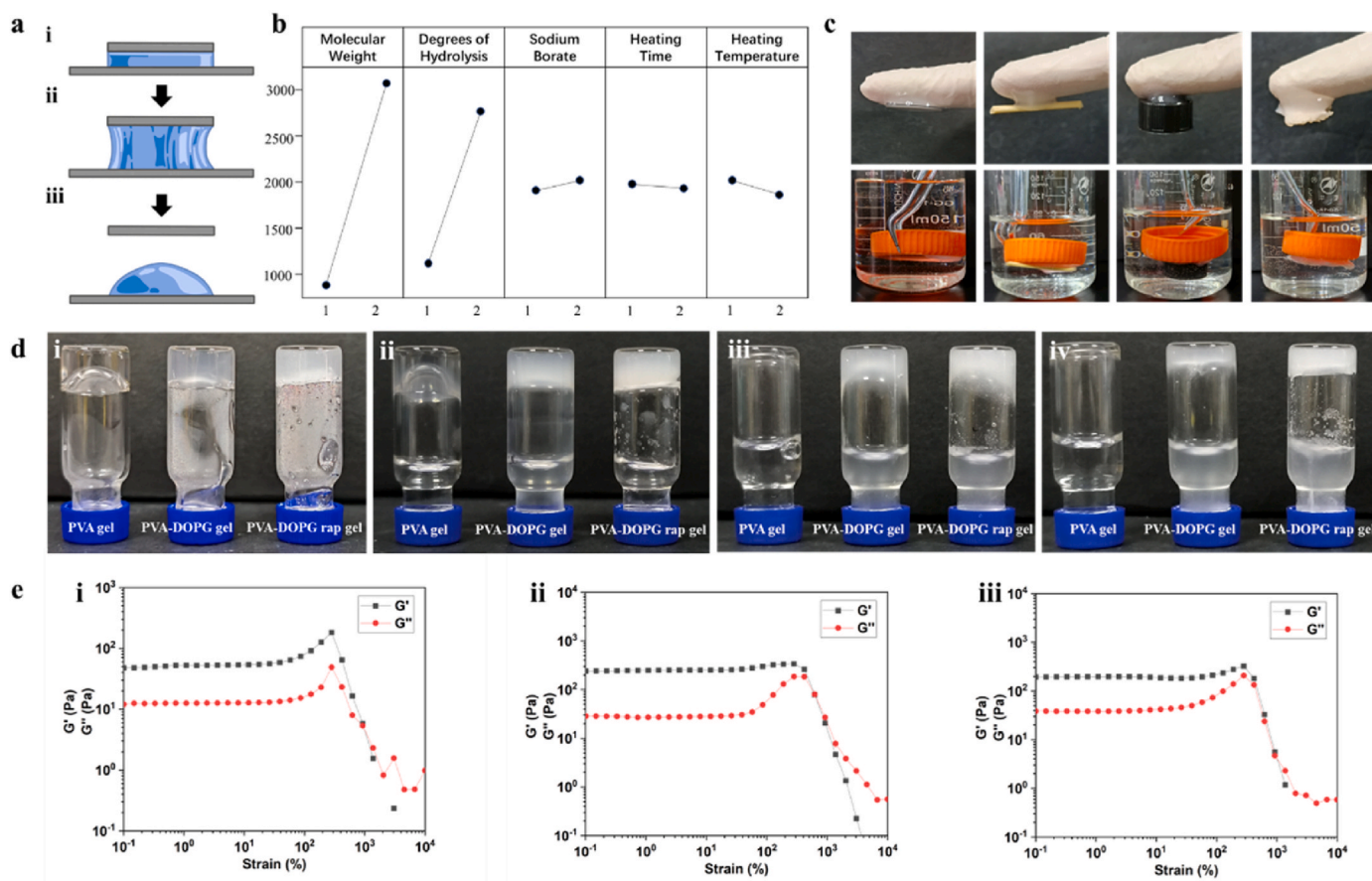
Fig. 2. Measurement of adhesiveness and characterization of PVA-DOPG hydrogels: (a) Schematic diagram of rheological tests to quantitatively measure adhesive force of hydrogels: (i) PP12 plate reaches at testing position; (ii) PP12 plate descends at first for a while and ascends at 1 μm/s and maximal normal force is recorded; (iii) PP12 plate keeps ascending till it is separated from hydrogels completely. (b) The effect plot of adhesive force. (c) PVA-DOPG rap hydrogels adhere to glass, woods, plastics and porcine buccal mucosa in the air and water. (d) PVA-DOPG hydrogels and PVA-DOPG rap hydrogels without PBS (i), in pH = 10 (ii), 7 (iii), 4 (iv) PBS. (e) Strain sweeps of PVA hydrogels (i), PVA-DOPG hydrogels (ii) and PVA-DOPG rap hydrogels (iii). Experiments were repeated at least three times.

distribution of drug molecules and adequate operating time. An adhesive hydrogel based on PVA polymer were established using PVA with a molecular weight of 146–186 kDa and 98 % degrees of hydrolysis, sodium borate (25 % volume ratio), a heating temperature of 90 °C, and a heating time of 10 min. According to that formulation, PVA-DOPG hydrogels were developed with an adhesive force of 6422.55 ± 1396.87 Pa, which was sufficient for adhering to mucosa without causing any discomfort during peeling. When loaded with rapamycin, although adhesive force of PVA-DOPG hydrogels decreases slightly (4431.94 ± 1174.96 Pa) ($p > 0.05$), they still adhered to various surfaces in both dry and wet conditions (Fig. 2c).

On the other hand, oral cavity is also a dynamic environment marked by fluctuating temperatures, near-neutral pH values, and high mechanical strain [37,38]. Hence, how those factors would impact the gelation of hydrogels are investigated. It was found that the gel-to-solution transition temperature of PVA-DOPG hydrogels was around 65 °C, which was higher than body temperature, suggesting that physiological temperatures did not hinder the gelation of the hydrogels (Appendix Table 5). The collapse of those hydrogels under different pH followed the order: basic pH < neutral pH < acidic pH (Fig. 2d), implying that pH significantly affects the gelation of hydrogels. Rheological strain sweep analysis revealed that the storage modulus (G') of PVA-DOPG hydrogels remained higher than the loss modulus (G'') when the strain exceeded 100 % (Fig. 2e), indicating their ability to withstand high strain. When loaded with rapamycin, response to temperature, pH, high strain of PVA-DOPG hydrogels remained nearly unchanged, demonstrating that addition of rapamycin did not significantly alter

those properties.

2.2. Enhanced penetration of PVA-DOPG hydrogels and mechanistic insights

Having demonstrated the adhesive properties of PVA-DOPG hydrogels, capable of adhering to diverse surfaces under dry and wet conditions, their potential to facilitate molecule penetration through the stratum corneum is yet to be unveiled. The hydrophilic stain fluorescein isothiocyanate (FITC) was uniformly distributed in both hydrogels, while the lipophilic stain nile red distributed uniformly in PVA-DOPG hydrogels but congregates in PVA hydrogels (Fig. 3a). Fluorescence of nile red was observed gradually crossing the stratum corneum of the porcine buccal mucosa (Fig. 3b). The integrated fluorescence density ($6.95 \pm 0.52 \times 10^6$) (Fig. 3c) and the fluorescence depth (0.96 ± 0.07 mm) (Fig. 3d) of PVA-DOPG hydrogels were significantly higher than those of the two others ($p < 0.001$), suggesting that PVA-DOPG hydrogels effectively promoted the penetration of lipophilic stains instead of hydrophilic molecules into isolated porcine buccal mucosa (Appendix Fig. 1).

Next, penetration across the cornified mucosa has been investigated. Red fluorescence emitted by hypericin was detected by VELscope (Fig. 3e). The mean fluorescence intensity of PVA-DOPG hydrogels was higher than that of poloxamer-HA hydrogels ($p < 0.01$) (Fig. 3f), indicating that PVA-DOPG hydrogels promote the penetration of hypericin across the cornified mucosa more effectively than commercial poloxamer hyaluronic acid (poloxamer-HA) hydrogels. Nevertheless, no
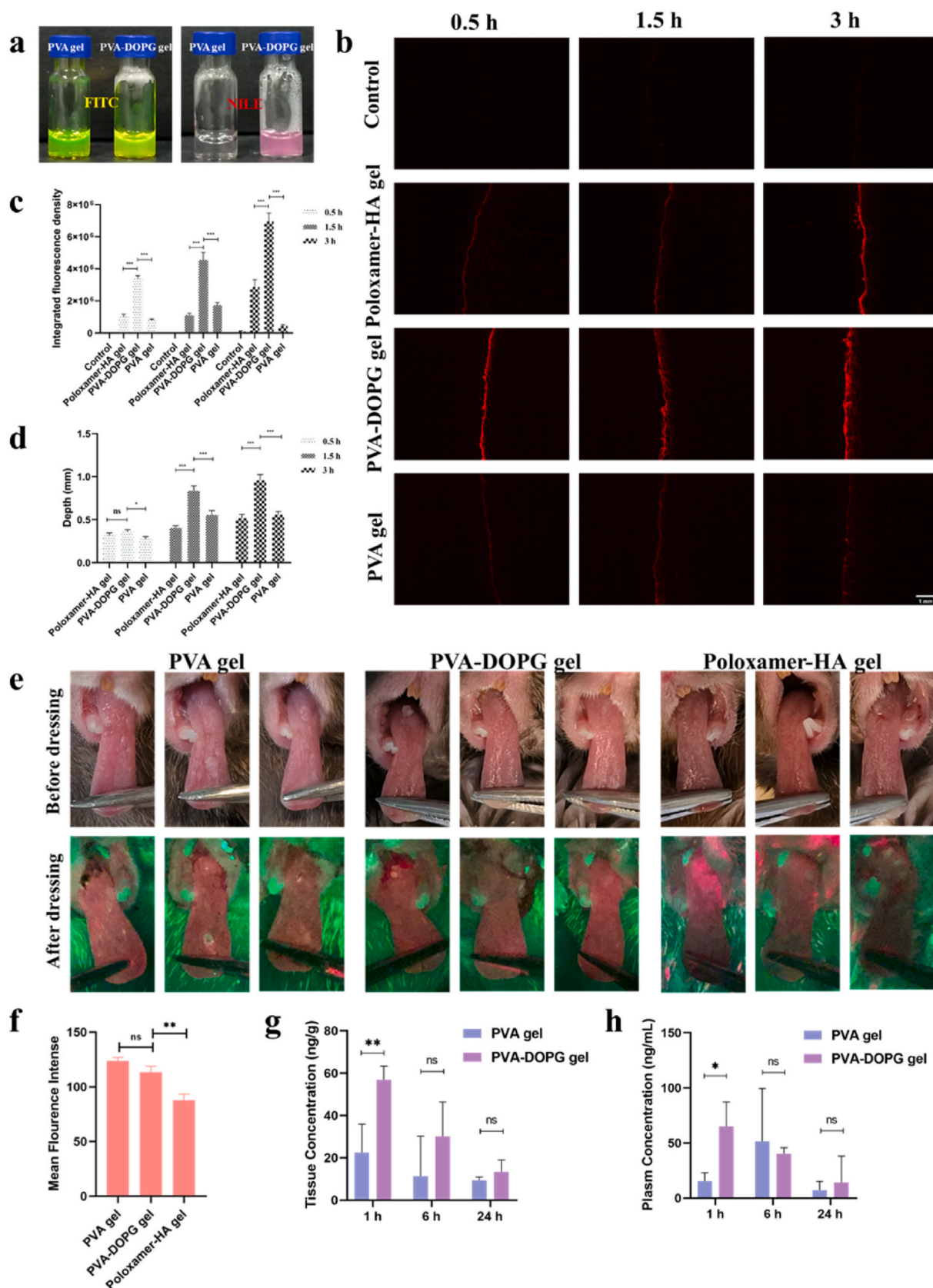
Fig. 3. *Promoted penetration of PVA-DOPG hydrogels: (a) Distribution of FITC and nile red in hydrogels. Frozen sections of porcine buccal mucosa (b) integrated fluorescence density (c) and fluorescence depth analysis (d). Pictures and VELscope images of cornified tongues (e) and analysis of the fluorescence (f). Rapamycin in tongues (g) and plasma (h) of PVA hydrogels group and PVA-DOPG hydrogels group. Experiments were repeated at least three times. The data were shown as the mean ± SEM. *p < 0.05, **p < 0.01, ***p < 0.001, ****p < 0.0001. (For interpretation of the references to colour in this figure legend, the reader is referred to the Web version of this article.)*

significant difference in mean fluorescence density was observed between PVA and PVA-DOPG hydrogels. This could be attributed to the constraints of VELscope, which detects fluorescence solely at the superficial layer, thereby complicating the accurate representation of the total amount of penetrated hypericin.

Then, penetration across the normal mucosa was investigated. Considering that the hydrogels may have been swallowed and would degrade in acidic digestive juice, the released molecules could be absorbed into the bloodstream through the gastrointestinal mucosa. The concentration of rapamycin both in tongue tissues and plasma have been compared after the local application of PVA-DOPG hydrogels loaded with rapamycin. The concentration of the PVA-DOPG hydrogels group in tongue tissues ($p < 0.01$) (Fig. 3g) and plasma ($p < 0.05$) (Fig. 3h) was significantly higher than that of the PVA hydrogel group at the first

hour, suggesting that PVA-DOPG hydrogels promoted the penetration of rapamycin more quickly.

All of the aforementioned results indicated that PVA-DOPG hydrogels significantly promoted the penetration of lipophilic molecules into the stratum corneum. To understand how PVA-DOPG hydrogels facilitate that penetration, the process was divided into three aspects: adhesion, release, and penetration. Quartz crystal microbalance with dissipation monitoring (QCMD) tests were performed to reveal adhesion and penetration. A decrease in frequency (F) and an increase in dissipation (D) indicated the formation of a mucus or lipid layer (Fig. 4a). The influx of PVA at high concentration led to further decreases in F and increases in D, suggesting an interaction between PVA and mucus (Fig. 4b–ii) or lipid (Fig. 4c–ii), although this interaction appeared to be weak and interrupted by water. On the other hand, the influx of PVA at
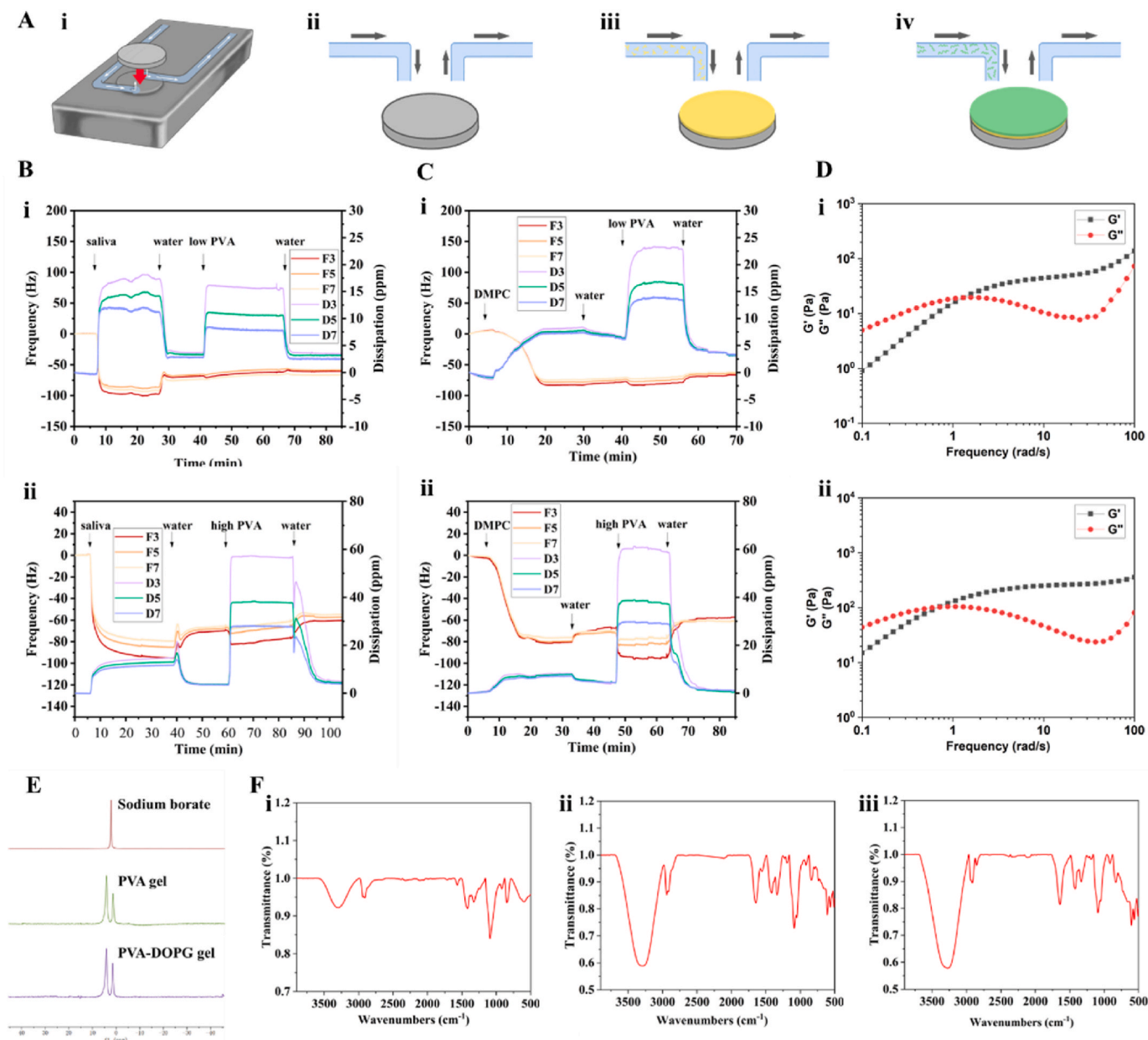
Fig. 4. Mechanism of penetration of PVA-DOPG hydrogels: (a) Scheme of a QCMD test: (i) possible passage way of influx and efflux of liquids; (ii) buffer influx to wet a crystal chip or flush weak connection; (iii) influx of saliva to establish a mucus layer and influx of dimyristoyl phosphatidylcholine (DMPC) vesicles to establish a lipid layer; (iv) influx of PVA solution to establish interaction with mucus or lipids. The tested process is: ii, iii, ii, iv, ii. (b) QCMD result of mucus with PVA in low concentration (i) and of mucus with PVA in high concentration (ii). (c) QCMD result of lipids with PVA in low concentration (i) and of mucus with PVA in high concentration (ii). (d) Frequency sweep of PVA (i) and PVA-DOPG (ii) hydrogels. (e) ^{11}B NMR spectra of sodium borate, PVA hydrogels and PVA-DOPG hydrogels. (f) FTIR spectra of PVA solution without borates (i), PVA hydrogels (ii) and PVA-DOPG hydrogels (iii). Experiments were repeated at least three times.

low concentration led to an increase in F with a mucus layer (Fig. 4b–i) and a decrease in F with a lipid layer (Fig. 4c–i), suggesting that PVA at low concentration did not interact with mucus but interacted with lipid, again with weak interaction. Rheological tests, nuclear magnetic resonance (NMR) tests and Fourier transform infrared spectroscopy (FTIR) were performed to reveal release. Furthermore, frequency sweep tests have showed that the storage modulus of hydrogels is lower than the loss modulus (Fig. 4d), indicating that the main connecting bonds are weak. NMR and FTIR spectra of PVA-DOPG hydrogels have indicated the

formation of boronic ester bonds, with a new peak (Fig. 4e) and characteristic absorption peak for B-O (absorption peak in 1050–1300 cm^{-1} and at 1050 cm^{-1}) (Fig. 4f) being observed.

2.3. Effect and mechanism of PVA-DOPG hydrogels loaded with rapamycin combating OLK malignant transformation

Following the verification that PVA-DOPG hydrogels enhance the penetration of lipophilic molecules into the stratum corneum, an
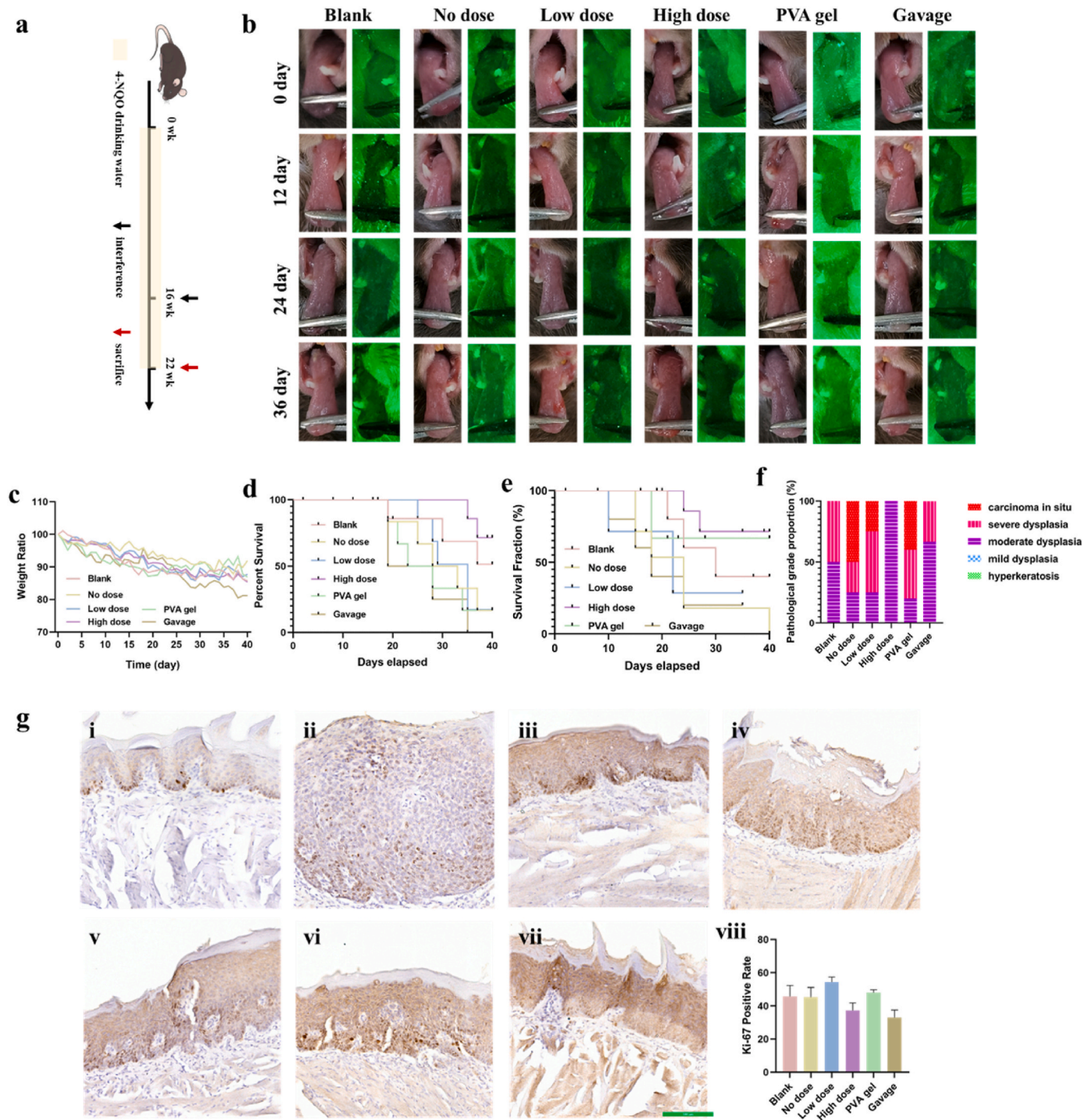
Fig. 5. Preventive effect of PVA-DOPG rap hydrogels (n = 54): (a) Scheme of establishing OLK mice model induced by 4-NQO. Pictures and VELscope images (b), weight analysis (c), survival analysis (d) and neoplasm analysis (e). (f) Pathological grade of those groups. (g) Ki-67 staining of normal tongues (i), blank group (ii), no dose group (iii), low dose group (iv), high dose group (v), PVA hydrogels (vi) and gavage group (vii) and statistical results (viii) (scale bar 1:100).

investigation was conducted to determine whether PVA-DOPG hydrogels loaded with rapamycin could inhibit OLK carcinogenesis. Prior to initiating the study on the anti-cancer efficacy, the biocompatibility of PVA-DOPG hydrogels was assessed. There were no evident macroscopic signs of local adverse reactions on the tongues during the application of hydrogels (Appendix Table 6). Histological examination of mouse tongues using hematoxylin and eosin (HE) staining, immunohistochemical staining for interleukin-6 (IL-6) and tumor necrosis factor-alpha (TNF-α) indicated no local adverse reactions (Appendix Fig. 2). No systemic adverse reactions were found by plasm biochemical index interested (Appendix Fig. 3) and HE staining of main internal organs (Appendix Fig. 4).

The reliability of the OLK mouse model induced by 4-Nitroquinoline N-oxide (4-NQO) in replicating the progression from potentially malignant lesions to carcinoma was then verified (Appendix Fig. 5). Macroscopic examination reveals the gradual appearance of rough tissues (12th week), white plaques (16th week), and neoplasm (18th week) on the tongues of the mice, accompanied by uneven autofluorescence intensities as the drinking time progresses. Histological analysis using HE staining demonstrated a gradual progression of hyperkeratosis, atypia, and invasive carcinoma. Immunohistochemical staining for Ki-67 reveals positive staining in epithelial cells that extends beyond the basal layer of the epithelium. Based on those findings, the OLK mouse model induced by 4-NQO successfully recapitulated the progression from OLK lesions to carcinoma.

Can PVA-DOPG hydrogels loaded with rapamycin (PVA-DOPG rap hydrogels) inhibit the progression of OLK to carcinoma? After 16 weeks of 4-NQO drinking water to establish the OLK model (Fig. 5a), hydrogels were applied daily for 6 weeks while continuing 4-NQO drinking water (considering that white-plaque lesions may disappear without drugs when 4-NQO drinking water was discontinued). Seven groups were divided: normal tongues (normal animals), blank group (OLK models without hydrogels or medication), no dose group (OLK models with PVA-DOPG hydrogels delivering no drugs), low dose group (OLK models with PVA-DOPG hydrogels delivering 5 mg/mL rapamycin), high dose group (OLK models with PVA-DOPG hydrogels delivering 25 mg/mL rapamycin) PVA hydrogels (OLK models with PVA hydrogels delivering 25 mg/mL rapamycin) and gavage group (OLK models with DOPG solution delivering 25 mg/mL rapamycin). Macroscopic examination of all groups was recorded (Fig. 5b). Body weight of the mice gradually decreases, with no significant difference being observed among the groups at the median time point ($p > 0.05$) (Fig. 5c), suggesting that 4-NQO led to weight loss and rapamycin did not reverse this effect. Survival analysis demonstrates that the high dose group had better survival rate than the other groups did ($p < 0.05$) (Fig. 5d), indicating that PVA-DOPG hydrogels carrying rapamycin in a high dose improved the survival of OLK mice. Analysis of neoplasm incidence shows that the high dose group had the lowest incidence of neoplasms, although without statistical significance ($p = 0.056$) (Fig. 5e). At the 40th day, the neoplasm incidence density (calculated as the number of new events divided by the total person-time at risk) of the blank group, no dose group, low dose group, high dose group, PVA hydrogels group, and gavage group is 0.0143 (95%CI: 0.0046, 0.0387), 0.024 (95%CI: 0.0098, 0.054), 0.0225 (95%CI: 0.0092, 0.0507), 0.0091 (95%CI: 0.0023, 0.0287), 0.0131 (95%CI: 0.0034, 0.041), and 0.0305 (95%CI: 0.0113, 0.0735), respectively. Compared with blank group, the neoplasm incidence density of high dose group has decreased by 36.36 %. Histological examination using HE staining is used to assess oral epithelial dysplasia (OED) (Appendix Fig. 6). OED of those groups were shown in Fig. 5f, which shows that PVA-DOPG hydrogels carrying rapamycin in a high dose effectively decreased the incidence of neoplasms. Immunohistochemical staining for Ki-67 analysis revealed that the high dose group has a positive rate of 37.33 ± 4.51 %, which was lower than the blank group (45.67 ± 6.66 %) ($p = 0.05$), lower than the no dose group (45.33 ± 5.77 %) ($p = 0.058$), significantly lower than the PVA hydrogels group (48 ± 1.73 %) ($p < 0.05$), and similar to the gavage group ($p > 0.05$)

(Fig. 5g). Those results suggested that PVA-DOPG hydrogels carrying rapamycin in a high dose inhibited the proliferation of epithelial cells.

The mechanism by which rapamycin inhibits OLK carcinogenesis was subsequently explored. Results of RNA sequencing revealed the up-regulation of 138 genes and the down-regulation of 427 genes in the rapamycin group compared to the normal group (Fig. 6a). Cluster analysis showed a good clustering pattern (Appendix Fig. 6). Kyoto Encyclopedia of Genes and Genomes (KEGG) analysis revealed that among the down-regulated genes, differentially expressed genes was the estrogen signaling (ER) pathway (Fig. 6b). Immunohistochemical staining of phosphorylated eIF4E-binding protein (p4EBP1) and phosphorylated S6 ribosomal protein (pS6) showed that expressions of the two downstream phosphorylated proteins of mTOR protein were down-regulated in the high-dose group (Fig. 6c). Western blot analyses revealed that proteins of pS6, Bcl-2, MMP-2 were down-regulated in response to rapamycin (Fig. 6d–Appendix Fig. 8); qPCR tests proved that rapamycin inhibited the gene expression of S6K1, Bcl-2, MMP-2 (Fig. 6e). All results above suggested that rapamycin might inhibit the malignant transformation via down-regulating the ER pathway.

3. Discussion

The responsiveness of hydrogels to acidic pH, high temperature and high strain can be attributed to the dynamic covalent bonds. The dynamic covalent bond utilized here is the boronic ester bond, formed by the interaction of sodium borate with 1,3-diol. Under alkaline conditions, the boron atom exhibits sp³ hybridization, which favors the formation of boronic ester bonds with cis-diol-containing compounds. Conversely, under acidic conditions, the boron atom undergoes a transition from sp³ to sp² hybridization, leading to the cleavage of the boronic ester bond [32,39]. Besides pH, temperature and mechanical force can also break chemical bonds [40–42]. Our experimental results demonstrate that PVA-DOPG hydrogels are sensitive to acidic pH, but insensitive to body temperature and high strain, indicating that acidity could promote the degradation of PVA-DOPG hydrogels in the oral cavity. Importantly, the pH of fresh human saliva typically ranges from 6.6 to 7.1, suggesting that the pH of saliva might trigger the degradation of hydrogels, leading to the release of drug molecules. It also denotes that isolation from saliva and the use of borates with lower pK_a values may delay the degradation of hydrogels based on boronic ester bonds.

Muco-adhesion and muco-penetration are two strategies employed to reach a more efficient mucosal drug delivery [43]. Muco-adhesion requires a strong interaction between mucus and particles, conversely, muco-penetration necessitates a weak interaction between mucus and particles. In our study, hydrogels are utilized as vehicles to provide sufficient retention time. Lipophilic molecules naturally repel water-containing mucus and attract lipid-containing stratum corneum. Based on QCMD results, it is inferred that PVA at high concentration is able to interact with mucus and provide adhesion force before PVA-DOPG hydrogels degrade. As the hydrogels degrade because of destruction of boronic ester bonds, PVA particles containing lipophilic molecules interact with the lipid layer, bringing lipophilic molecules closer to the stratum corneum and facilitating their passive diffusion into the stratum corneum. Additionally, the incorporation of DOPG promotes the penetration of lipophilic molecules, which may be attributed to the uniform distribution of lipophilic molecules within the hydrogels and the potential role of DOPG as a penetration enhancer [44, 45].

Rapamycin shows significant anti-cancer effect in 4-NQO induced mice models and is revealed to be related to estrogen signaling pathway. The estrogen signaling pathway has been found to be activated in multiple cancers [46]. It has been reported that estrogen receptor (ER) is present in some head and neck squamous cell carcinoma (HNSCC) patients and is negatively correlated with prognosis [47,48]. Furthermore, estrogen has been shown to promote the proliferation of HNSCC cells, and knock-down of ER inhibits the proliferation of these cells [49,50].
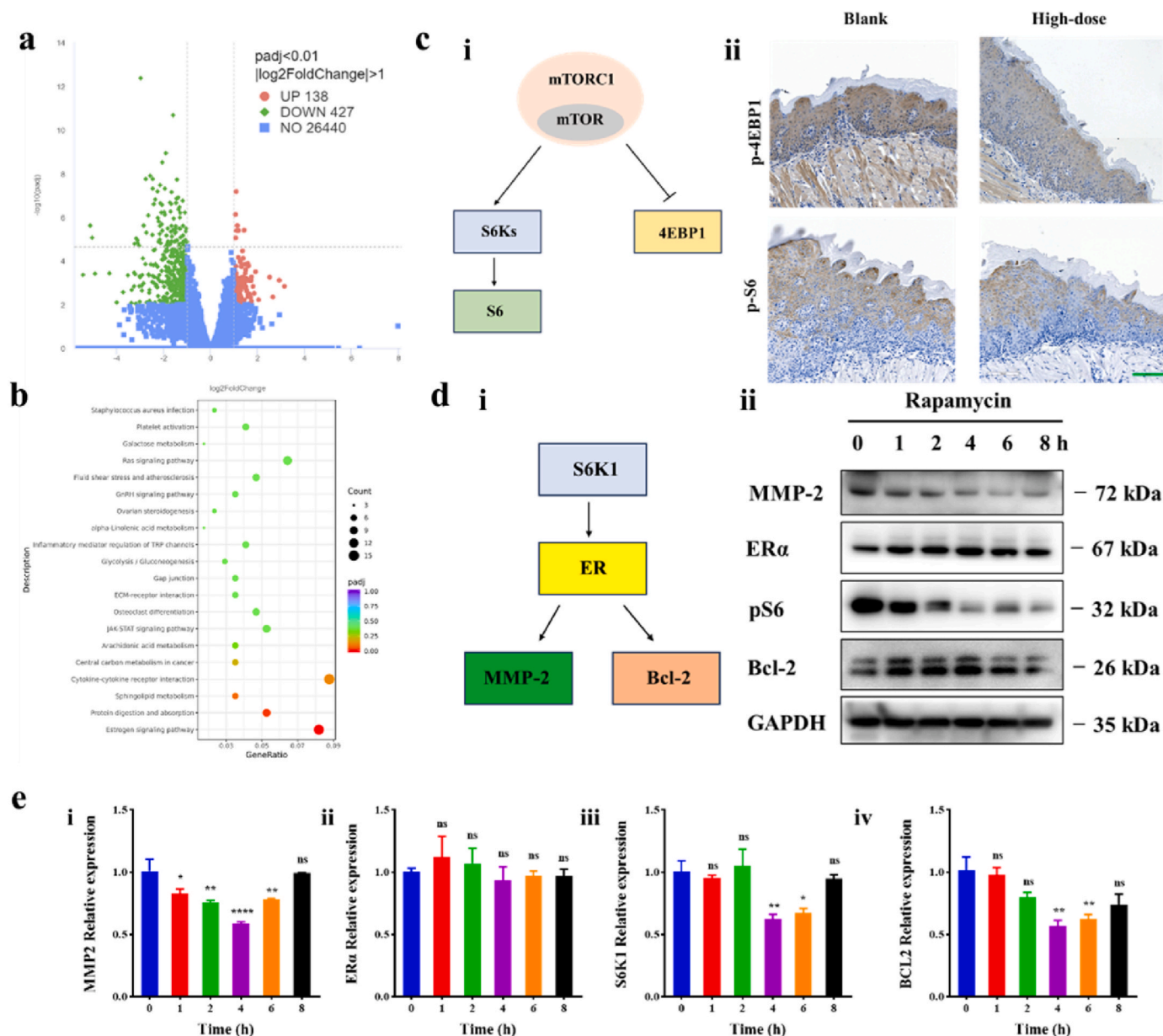
Fig. 6. Mechanism of rapamycin inhibiting carcinogenesis: (a) Volcano plot of mice tongues in blank and rapamycin group. (b) KEGG analysis of down-regulated genes. (c) Diagram of mTORC1 regulate S6K and 4EBP1 (i) and immunohistochemical staining of and pS6 in blank and high-dose group (scale bar 1:100) (ii). (d) Diagram of S6K1 regulates ER, MMP-2 and Bcl-2 (i) and Western blotting results of HSC-3 cell line after rapamycin processing (ii). (e) qPCR results of HSC-3 cell line after rapamycin processing. Experiments were repeated at least three times.

Rapamycin, by binding to FK506-binding protein of 12 kDa (FKBP12), inhibits the activity of mTORC1, which phosphorylates ribosomal protein S6 kinase 1 (S6K1) [51,52]. S6K1 has been reported to phosphorylate Ser167 of ERα, thereby promoting its transcription [53,54]. Rapamycin can reverse this process. It is inferred that rapamycin inhibits OLK from carcinogenesis by down-regulating the estrogen signaling pathway. But further investigation is required to establish the relationship between rapamycin and the estrogen signaling pathway, as well as to elucidate the precise mechanisms through which rapamycin interacts with this pathway. In our study, RNA sequencing was performed on a complete tongue tissue, comprising epithelium, connective tissue, and muscles, which could potentially affect the sequencing results. To enhance the accuracy of future experiments, it is recommended to carefully isolate the epithelium before conducting RNA sequencing and subsequent analyses.

By the way, a recent study by Hanna et al. demonstrated the potential

clinical activity of nivolumab (480 mg intravenously), an inhibitor of the programmed cell death 1 protein (PD-1), in an immune checkpoint therapy trial for high-risk OLK [55]. However, immune-related adverse events remind that local administration of nivolumab may hold greater promise in reducing both the required dosage and associated toxicity, when compared to intravenous administration. Meanwhile, this PVA-DOPG drug delivery system only contains carbon, hydrogen, oxygen, nitrogen, phosphorus and boron. No heavy metals are involved. Raw materials of PVA and DOPG are all renewable. As what mentioned above, PVA-DOPG hydrogels cause no local adverse reactions or systemic adverse reactions. Thus, PVA-DOPG hydrogel delivery system is rather environmentally friendly, sustainable and biocompatible.

4. Conclusions

In our study, considering the wetness, functions, dynamics, and

barriers of oral cavity, PVA-DOPG hydrogels integrating adhesion and lipophilicity have been developed for loading rapamycin, aiming to inhibit the malignant transformation of OPMD. The adhesion of PVA-DOPG hydrogels is optimized to reach an ideal adhesive force of 6 kPa and adhere to various surfaces and the lipophilicity of the hydrogels is illustrated by lipophilic molecules' more uniform distribution and more enhanced penetration into stratum corneum (integrated fluorescence density of $6.95 \pm 0.52 \times 10^6$ and mean fluorescence depth of 0.96 ± 0.07 mm) ($p < 0.001$). By incorporating rapamycin, biocompatible PVA-DOPG hydrogels have exhibited a significant effect in inhibiting the malignant transformation of 4-NQO induced OPMD mice animals (the neoplasm incidence density at the 40th day is 0.0091) ($p < 0.05$), decrease in neoplasm incidence density of 36.36 % and inhibition rate in neoplasm volume of 75.04 ± 33.67 %).

Besides what mentioned above that PVA-DOPG hydrogel delivered rapamycin for OLK management which showed potential as a local delivery system for lipophilic drugs especially on condition that adhesion is needed. Also, it has potential as a wound dressing which protect skin and mucosa from the external environmental aggressions, shield the body from physical, biological, and chemical damage. However, usage is limited in extreme acidic environment like gastric mucosal lesions.

5. Materials and methods

5.1. Materials

PVA (Cas NO. 9002-89-5) with different molecular weight and degrees of hydrolysis were purchased from Sigma. DOPG (Cas NO. 62700-69-0) (TCI, Japan), rapamycin (Cas NO. 53123-88-9) (Shaosu, China), nile red (Cas NO. 7385-67-3) (sigma, the USA), FITC (Cas NO. 3326-32-7) (Adamas, China), artificial saliva (Solarbio, China), hypericin (Cas NO. 548-04-9) (Bide medication, China), 4-NQO (Cas NO. 56-57-5) (TCI, Japan), Poloxamer-HA (ALA, China), dimyristoyl phosphatidylcholine (DMPC) (Cas NO. 18194-24-6) (A.V.T,China), anti Ki-67 antibody (abcam, British), anti IL-6 antibody (abcam, British), anti TNF-α antibody (Abcam, British) were purchased from the corresponding companies.

Male C57BL/6JGpt mice were purchased from Jicuiyaokang Biotechnology Co., Ltd (Jiangsu, China). All experiments were conducted in accordance with the guidelines outlined in the ''Principles of Laboratory Animal Care'' (NIH) and were approved by the Ethics Committee of West China Hospital of Stomatology, Sichuan University. The animals had free access to sterilized/4-NQO water and food in a temperature-controlled room (22 °C) with a 12 h light/dark cycle. They were fed adaptively for one week in these surroundings before the experiments.

5.2. Orthogonal experiment and adhesion measurement

PVA powder (0.88 g) was heated in ultra-pure water (20 mL) till all powder was dissolved completely to make PVA solution. Equal sodium hydroxide (0.5 M) and boric acid (0.5 M) were mixed to make sodium borate (0.25 M) and was diluted ten-fold (0.025 M). Varied PVA solution (1 mL) and sodium borate (200 μL or 500 μL) were mixed, heated (80 °C or 90 °C) for a while (5 min or 10 min). Those hydrogels in liquid status were poured onto the parallel plate of rheometer (Anton Paar, Germany). PP12 plate (S = 0.011 m^2) descends and compresses hydrogels. Excessive hydrogels were extruded till remaining hydrogels reach at 1 mm in thickness. Extruded hydrogels were scraped off. Test was started after 5 min. Maximal normal force (F) was recorded and adhesion force (p) was calculated as p = F/S.

5.3. Preparation of hydrogels

DOPG powder (400 mg) was dissolved in sodium borate (0.025 M, 20 mL) at room temperature to make milk-like DOPG solution. DOPG solution, PVA solution and sodium borate were mixed as $V_{(DOPG)}$: $V_{(PVA)}$: $V_{(sodium\ borate)} = 1$: 2: 1, heated for 10 min (90 °C) and cooled down at room temperature for over 5 min to make PVA-DOPG hydrogels. Rapamycin was added to DOPG solution and vortexed. DOPG solution with rapamycin, PVA solution and sodium borate were mixed as $V_{(DOPG\ and\ rapamycin)}$: $V_{(PVA)}$: $V_{(sodium\ borate)} = 1$: 2: 1, heated for 10 min (90 °C) and cooled down at room temperature for over 5 min to make PVA-DOPG rap hydrogels. Ultra-pure water, PVA solution and sodium borate and were mixed as $V_{(water)}$: $V_{(PVA)}$: $V_{(sodium\ borate)} = 1$: 2: 1, heated for 10 min (90 °C) and cooled down at room temperature for over 5 min to make PVA hydrogels.

5.4. Vial inversion tests

According to the formulation and parameters above, hydrogels were developed in a vial and the vial is inverted. If hydrogels resisted gravity and keeps status of solid, successful vial inversion (SVI) was determined. Contrarily, if hydrogels did not resist gravity and cannot keeps status of solid after interference, unsuccessful vial inversion (UVI) was determined. Lifetime stability was calculated from when hydrogels were developed to when gels crystallize or UVI. Thermal reversibility was decided when hydrogels was heated again to be liquid and then cool down with SVI. Concentration of PVA was not calculated until UVI with extra ultra-pure water being added (100 μL per time) into hydrogels (200 μL) and heating-cooling cycling. Hydrogels (400 μL) were formed in a vial and PBS (400 μL) at different pH was added onto the gels. Vial inversion tests were performed 1 h later to decide SVI or UVI and remaining gels were recorded.

5.5. Penetration ability tests

Firstly, fresh isolated normal porcine buccal mucosa was bought from local butcher and trimmed to be rectangle with similar width and length. Hydrogels carrying nile red or FITC were applied onto the mucosa and the tissue was fixed onto a slide via a thin ribbon. That slide was immersed into artificial saliva who is heated to keep at 37 °C with the rotator spinning at 200 rpm. Those buccal tissues were frozen by dry ice and embedded into OCT. Slices were made with 30 μm thickness and observed under microscope (Olympus, Japan). Images were dealt with ImageJ software and analyzed via SPSS statistics 26 software. Secondly, male C57BL/6JGpt mice (GemPharmatech, China) were fed with 4-NQO drinking water (50 μg/mL) for about 16 weeks. Hypericin (30 mg) was added to DOPG solution (500 μL) or ultra-pure water (500 μL) and vortexed. As what mentioned above, PVA-DOPG hydrogels carrying hypericin and PVA hydrogels carrying hypericin were developed respectively. Thermal-sensitive poloxamer-HA hydrogels were provided by ALA cooperation. Poloxamer-HA hydrogels were in liquid status at 4 °C and turned to be solid status at room temperature. Hypericin (30 mg) was mixed with poloxamer-HA hydrogels (500 μL) on ice and vortexed. Poloxamer-HA hydrogels carrying hypericin were stored at room temperature for later use. Those three hydrogels (100 μL) were applied on mice tongue for 1.5 h with mice being anesthetized. New application (100 μL) was followed for another 1.5 h. VELscope images were captured before and after application, which were dealt with ImageJ software and analyzed via SPSS software. Blank group was untreated. Every group has 3 mice and a total of 12 mice were used. Simple size was determined based on references.

Thirdly, PVA-DOPG rap hydrogels (200 μL) and PVA rap hydrogels (200 μL) were applied on normal male C57BL/6JGpt mice tongue tissues for once. Every group has 9 mice and a total of 9 mice were used. Simple size was determined based on references. Tongues tissues and blood were collected for further rapamycin detection by high-performance liquid chromatograph (Shimadzu, Japan).

5.6. Collection of fresh saliva and formation of DMPC vesicles and QCMD tests

This study was approved by the Ethics Committee of West China Hospital of Stomatology, Sichuan University (WCHSIRB-CT-2021-338). Centrifuge tubes (50 mL) was pressed close to lower lip of volunteers with head down forward. Fresh saliva outflowed into the tube and stored at 4 °C for later use. DMPC powder (20 mg) was dissolved with chloroform and dried under a stream of nitrogen. Being kept under vacuum overnight, the dried lipid film was resuspended in ultra-pure water (20 mL) at 35 °C. Next, the solution was sonicated with a probe tip sonicator (Scientz, China) till the milky solution turns to be clear. QCMD is a label-free mass-adsorption technique at solid-liquid interface which can help to understand binding processes based on changes in the frequency and dissipation. In our study, a QCMD technique (Biolin Scientific, Sweden) was used. Fresh saliva vesicles underwent surface adsorption onto SiO_2-coated quartz crystal sensors to form a mucus layer and DMPC to form a lipid bilayer. Fresh saliva or DMPC vesicles were injected into the QCM chamber at a flow rate of 100 μL/min using a peristaltic pump at 37 °C.

5.7. NMR tests and FTIR tests

Considering that PVA (molecular weight: 146–186 kDa; degrees of hydrolysis: 98 %) in high concentration form solid gel with sodium borate at the lowest concentration detected by NMR. Therefore, PVA (molecular weight: 13–23 kDa; degrees of hydrolysis: 88 %) and 0.25 M sodium borate were chosen to form PVA-DOPG solution. D_2O was added into PVA-DOPG solution to make 10 % volume fraction. NMR spectra were recorded on a spectrometer (AV II, Germany) at 600 MHz and ^{11}B NMR signals were detected. PVA-DOPG hydrogels were frozen and evaporated using a vacuum pump. The xerogels were scanned in a FTIR spectrometer (Bruker, Germany) through 400 to 4000 cm^{-1} scanning ranges for 16 times and 4 cm^{-1} resolution.

5.8. PVA-DOPG rap hydrogels applied in OLK and RNA sequencing

This study was approved by the Ethics Committee of West China Hospital of Stomatology, Sichuan University (WCHSIRB-D-2023-274). Male C57BL/6JGpt mice were fed with 4-NQO (50 μM) for 16 weeks to establish OLK models. Mice are divided into 6 groups randomly. Every group has 9 mice and a total of 54 mice were used. Blank group was untreated. Simple size was determined based on references. No dose group, low dose group and high dose group were treated with PVA-DOPG hydrogels carrying rapamycin at 0 mg/mL, 2.5 mg/mL and 12.5 mg/mL. PVA group was treated with PVA hydrogels carrying rapamycin at 12.5 mg/mL. Gavage group was treated with DOPG solution carrying rapamycin at 12.5 mg/mL. Interference was applied once a day. The position of mouse cage, the order of treatment and measurements were randomly assigned every day. Weight of mice, survival and papilloma were recorded every day. Decrease of weight loss exceeded 20 % were euthanized. Five mice tongues in each group were embedded by paraffin and taken to stain HE, Ki-67, IL-6 and TNF-α. Degrees of dysplasia were determined by three seasoned pathologists in blind experiments.

Four mice tongues in control group and high-dose group were collected respectively and sent to Novogene cooperation for RNA sequencing. Data was analyzed on NovoMagic with log_2Fold Change >1 and *p* adjusted <0.01. Clustering analysis, GO analysis and KEGG analysis were performed.

5.9. PVA-DOPG rap hydrogels applied in tumor

Male C57BL/6JGpt mice were fed with 4-NQO (50 μM) for 18 weeks to establish tumor models. Mice are divided into 6 groups randomly. Blank group was untreated. Every group has 6 mice and a total of 18 mice were used. Simple size was determined based on references. PVA hydrogels group was treated with PVA hydrogels carrying rapamycin at 12.5 mg/mL. PVA-DOPG hydrogels group was treated with PVA-DOPG hydrogels carrying rapamycin at 12.5 mg/mL. Interference was applied once a day. The position of mouse cage, the order of treatment and measurements were randomly assigned every day. Papilloma was measured. Male C57BL/6JGpt mice were fed with 4-NQO (50 μM) for 16 weeks to establish OLK models. Blank group was untreated. Rapamycin group was treated with PVA-DOPG hydrogels carrying rapamycin at 12.5 mg/mL. Decrease of weight loss exceeded 20 % were euthanized.

5.10. Quantitative real-time PCR

HSC-3 cells in 6-well plates were treated with control, rapamycin (100 nM) for 1 h, 2 h, 4 h, 6 h and 8 h, respectively. Then, total RNA was extracted (FOREGENE) and reverse transcribed into cDNA (TaKaRa). Finally, qRT-PCR was performed using the TB Green® PreMix EX Taq™ II Kit (TaKaRa). The following primer pairs were used for quantitative qRT-PCR: human ERα, 5′- GCTTACTGACCAACCTGGCAGA-3′ (forward), 5′-GGATCTCTAGCCAGGCACATTC-3′ (reverse); human BCL2, 5′-ATCGCCCTGTGGATGACTGAGT-3′ (forward), 5′-GCCAGGA-GAAATCAAACAGAGGC-3′ (reverse); human MMP2, 5′- AGCGAGTG-GATGCCGCCTTTAA-3′ (forward), 5′- CATTCCAGGCATCTGCGATGAG-3′ (reverse); human S6K1, 5′-TATTGGCAGCCCACGAACACCT-3′ (forward), 5′-GTCACATCCATCTGCTCTATGCC-3′ (reverse); human GAPDH, 5′-CAGGAGGCATTGCTGATGAT-3′ (forward), 5′-GAAGGCTGGGGCTCATTT-3′ (reverse).

5.11. Western blot

HSC-3 cells in 6-well plates were treated with control, rapamycin (20 nM) for 1 h, 2 h, 4 h, 6 h and 8 h, respectively. The total cell lysates were obtained in RIPA Lysis Buffer (Beyotime, with protease and phosphatase inhibitor cocktail) and quantified by Micro BCA Protein Assay Kit (CWBIO, CW2011S). Then western blot was conducted as described previously [34]. The samples were subjected to 12 % sodium dodecyl sulfate polyacrylamide hydrogel electrophoresis (SDS-PAGE) at 120 V for 1 h and then transferred onto 0.22 μm polyvinylidene difluoride membranes (PVDF, MA, USA) using wet transfer electrophoresis at 300 mA for 1.5 h. The membranes were blocked with 5 % nonfat milk in TBST for 1 h at room temperature and then incubated with diluted primary antibodies (rabbit antibodies including ERα, Proteintech, Cat No: 21244-1-AP, 1/1000, MMP2, Proteintech, Cat No: 10373-2-AP, 1/800, Phospho-S6 Ribosomal Protein (Ser235/236), CST, Cat No: 4858, 1/2000, BCL2, abcam, Cat No: ab182858, 1/2000, GAPDH, Proteintech, Cat No: 10494-1-A5000P, 1/) at 4 °C with gentle shaking, overnight. After washing with TBST, membranes were incubated with secondary antibody (Rabbit, ZSGB-BIO, ZB2306, 1/5000) for 2 h at room temperature. Finally, the membranes were exposed using Immobilon® Western Chemiluminescent HRP Substrate.

Statistical analysis

Data were analyzed by IBM SPSS Statistics 26 software using the Mann–Whitney test, Fischer precision test one-way ANOVA. The data were expressed as mean ± SEM or mean ± SD. (ns: no statistical significance, *p < 0.05, **p < 0.01, ***p < 0.001, ****p < 0.0001)

CRediT authorship contribution statement

Yuqi Du: Writing – review & editing, Writing – original draft, Visualization, Software, Methodology, Formal analysis, Data curation. **Tiannan Liu:** Methodology, Investigation, Formal analysis, Data curation. **Tingting Ding:** Methodology, Funding acquisition, Formal analysis, Data curation. **Xin Zeng:** Validation, Supervision, Resources, Project administration, Funding acquisition. **Qianming Chen:** Validation, Supervision, Resources, Project administration, Funding

acquisition. **Hang Zhao:** Validation, Supervision, Project administration, Funding acquisition, Conceptualization.

Declaration of competing interest

The authors declare that they have no known competing financial interests or personal relationships that could have appeared to influence the work reported in this paper.

Acknowledgments

Appendix A. Supplementary data

Supplementary data to this article can be found online at https://doi.org/10.1016/j.mtbio.2024.101305.

Data availability

Data will be made available on request.

References

[1] J.M. Aguirre-Urizar, I. Lafuente-Ibáñez de Mendoza, S. Warnakulasuriya, Oral Dis. 27 (2021) 1881–1895.
[2] G.A. Scardina, F. Carini, E. Maresi, V. Valenza, P. Messina, Methods Find Exp Clin Pharmacol 28 (2006) 115–119.
[3] M.A. Kuriakose, K. Ramdas, B. Dey, S. Iyer, G. Rajan, K.K. Elango, A. Suresh, D. Ravindran, R.R. Kumar, P. R, S. Ramachandran, N.A. Kumar, G. Thomas, T. Somanathan, H.K. Ravindran, K. Ranganathan, S.B. Katakam, S. Parashuram, V. Jayaprakash, M.R. Pillai, Cancer Prev. Res. 9 (2016) 683–691.
[4] B. Luiza Koop, M. Nascimento da Silva, F. Diniz da Silva, K. Thayres Dos Santos Lima, L. Santos Soares, C. Jose de Andrade, G. Ayala Valencia, A. Rodrigues Monteiro, Food Res. Int. 153 (2022) 110929.
[5] A.E.M. Marques, G.A. Borges, C.H. Viesi do Nascimento Filho, L.M.S. Vianna, D. Ramos, R.M. Castilho, C.H. Squarize, E.N.S. Guerra, Oral Surg Oral Med Oral Pathol Oral Radiol 133 (2022) 453–461.
[6] K. Tashiro, M. Oikawa, Y. Miki, T. Takahashi, H. Kumamoto, Odontology 108 (2020) 91–101.
[7] A. Bouyahya, A. El Allam, S. Aboulaghras, S. Bakrim, N. El Menyiy, M. M. Alshahrani, A.A. Al Awadh, T. Benali, L.H. Lee, N. El Omari, K.W. Goh, L. C. Ming, M.S. Mubarak, Cancers 14 (2022).
[8] J. Patel, S.A. Nguyen, B. Ogretmen, J.S. Gutkind, C.A. Nathan, T. Day, Laryngoscope Investig Otolaryngol 5 (2020) 243–255.
[9] C. Harsha, K. Banik, H.L. Ang, S. Girisa, R. Vikkurthi, D. Parama, V. Rana, B. Shabnam, E. Khatoon, A.P. Kumar, A.B. Kunnumakkara, Int. J. Mol. Sci. 21 (2020).
[10] S. Stanciu, F. Ionita-Radu, C. Stefani, D. Miricescu, S. Stanescu II, M. Greabu, A. Ripszky Totan, M. Jinga, Int. J. Mol. Sci. 23 (2022).
[11] P. Zhang, L. Zhang, X.J. Yue, Y.J. Tang, C. Wu, Y.Z. Li, Appl. Microbiol. Biotechnol. 104 (2020) 9125–9134.
[12] V. Hurez, V. Dao, A. Liu, S. Pandeswara, J. Gelfond, L. Sun, M. Bergman, C. J. Orihuela, V. Galvan, A. Padron, J. Drerup, Y. Liu, P. Hasty, Z.D. Sharp, T. J. Curiel, Aging Cell 14 (2015) 945–956.
[13] E. Landh, L.M. Moir, L. Gomes Dos Reis, D. Traini, P.M. Young, H.X. Ong, Eur J Pharm Sci 142 (2020) 105098.
[14] Y. Komagamine, M. Kanazawa, A. Yamada, S. Minakuchi, Aging Clin. Exp. Res. 31 (2019) 1243–1248.
[15] A.V. Amerongen, E.C. Veerman, Oral Dis. 8 (2002) 12–22.
[16] S. Li, H. Zhang, K. Chen, M. Jin, S.H. Vu, S. Jung, N. He, Z. Zheng, M.S. Lee, Drug Deliv. 29 (2022) 1142–1149.

[17] J.G. Edmans, C. Murdoch, M.E. Santocildes-Romero, P.V. Hatton, H.E. Colley, S. G. Spain, Mater Sci Eng C Mater Biol Appl 112 (2020) 110917.
[18] X. Du, N. Gao, X. Song, Drug Deliv. 28 (2021) 252–260.
[19] R.H. Schmedlen, K.S. Masters, J.L. West, Biomaterials 23 (2002) 4325–4332.
[20] L. Chen, B. Zheng, Y. Xu, C. Sun, W. Wu, X. Xie, Y. Zhu, W. Cai, S. Lin, Y. Luo, C. Shi, J Nanobiotechnology 21 (2023) 202.
[21] T. Fang, X. Cao, B. Shen, Z. Chen, G. Chen, Biomaterials 300 (2023) 122189.
[22] J. Meng, X. Yang, J. Huang, Z. Tuo, Y. Hu, Z. Liao, Y. Tian, S. Deng, Y. Deng, Z. Zhou, J.F. Lovell, H. Jin, Y. Liu, K. Yang, Adv. Sci. (2023) e2300517, https://doi.org/10.1002/advs.202300517.
[23] M.U.A. Khan, Z. Yaqoob, M.N.M. Ansari, S.I.A. Razak, M.A. Raza, A. Sajjad, S. Haider, F.M. Busra, Polymers 13 (2021).
[24] M.U.A. Khan, I. Iqbal, M.N.M. Ansari, S.I.A. Razak, M.A. Raza, A. Sajjad, F. Jabeen, M. Riduan Mohamad, N. Jusoh, Molecules 26 (2021).
[25] L. Serairi, C. Santillo, P. Basset, M. Lavorgna, G. Pace, Adv. Mater. 36 (2024).
[26] P.P. de Oliveira, V.P. Bavaresco, L.M. Silveira-Filho, A.A. Schenka, K.A. Vilarinho, E.S. Barbosa de Oliveira Severino, O. Petrucci, J. Thorac. Cardiovasc. Surg. 147 (2014) 1405–1410.
[27] Y. Mu, X. Wan, Macromol. Rapid Commun. 37 (2016) 545–550.
[28] H. Zhu, J. Xu, M. Zhao, H. Luo, M. Lin, Y. Luo, Y. Li, H. He, J. Wu, Front. Bioeng. Biotechnol. 10 (2022) 968078.
[29] A.D. Postle, E.L. Heeley, D.C. Wilton, Comp. Biochem. Physiol. Mol. Integr. Physiol. 129 (2001) 65–73.
[30] S. Preuss, J. Scheiermann, S. Stadelmann, F.D. Omam, S. Winoto-Morbach, D. Lex, P. von Bismarck, S. Adam-Klages, F. Knerlich-Lukoschus, D. Wesch, J. Held-Feindt, S. Uhlig, S. Schutze, M.F. Krause, Pulm. Pharmacol. Ther. 28 (2014) 25–34.
[31] O.R. Cromwell, J. Chung, Z. Guan, J. Am. Chem. Soc. 137 (2015) 6492–6495.
[32] D. Li, Y. Chen, Z. Liu, Chem. Soc. Rev. 44 (2015) 8097–8123.
[33] X.T. Zhang, G.J. Liu, Z.W. Ning, G.W. Xing, Carbohydr. Res. 452 (2017) 129–148.
[34] H. Zhao, H. Feng, J. Liu, F. Tang, Y. Du, N. Ji, L. Xie, X. Zhao, Z. Wang, Q. Chen, Biomaterials 230 (2020) 119598.
[35] J. Qi, T. Ding, T. Liu, X. Xia, S. Wu, J. Liu, Q. Chen, D. Zhang, H. Zhao, Adv. Funct. Mater. 32 (2022).
[36] T. Ding, J. Zou, J. Qi, H. Dan, F. Tang, H. Zhao, Q. Chen, J. Dent. Res. 101 (2022) 921–930.
[37] V. Raja, S.R. Priyadarshini, J.A. Moses, C. Anandharamakrishnan, Food Funct. 13 (2022) 10426–10438.
[38] S.P. Cocksedge, A.J. Causer, P.G. Winyard, A.M. Jones, S.J. Bailey, Nutrients 15 (2023).
[39] X.Q. Xie, Y. Zhang, Y. Liang, M. Wang, Y. Cui, J. Li, C.S. Liu, Angew Chem. Int. Ed. Engl. 61 (2022) e202114471.
[40] G.S. Han, D.W. Domaille, J. Mater. Chem. B 10 (2022) 6263–6278.
[41] S. Liu, Z. Du, P. Li, F. Li, Biosens. Bioelectron. 35 (2012) 443–446.
[42] B. Marco-Dufort, J.R. Janczy, T. Hu, M. Lutolf, F. Gatti, M. Wolf, A. Woods, S. Tetter, B.V. Sridhar, M.W. Tibbitt, Sci. Adv. 8 (2022) eabo0502.
[43] K. Netsomboon, A. Bernkop-Schnurch, Eur. J. Pharm. Biopharm. 98 (2016) 76–89.
[44] S. Narasimha Murthy, Y.L. Zhao, S.W. Hui, A. Sen, Int J Pharm 326 (2006) 1–6.
[45] J. Lee, M. Noh, J. Jang, J.B. Lee, Y.H. Hwang, H. Lee, ACS Appl. Mater. Interfaces 14 (2022) 36331–36340.
[46] S. Chaturantabut, A. Shwartz, K.J. Evason, A.G. Cox, K. Labella, A.G. Schepers, S. Yang, M. Acuna, Y. Houvras, L. Mancio-Silva, S. Romano, D.A. Gorelick, D. E. Cohen, L.I. Zon, S.N. Bhatia, T.E. North, W. Goessling, Gastroenterology 156 (2019) 1788–1804 e1713.
[47] Y.L. Chang, Y.K. Hsu, T.F. Wu, C.M. Huang, L.Y. Liou, Y.W. Chiu, Y.H. Hsiao, F. J. Luo, T.C. Yuan, Endocr. Relat. Cancer 21 (2014) 555–565.
[48] K. Grsic, I.L. Opacic, S. Sitic, M. Milkovic Perisa, P. Suton, B. Sarcevic, Oncol. Lett. 12 (2016) 3861–3865.
[49] V. Drake, E. Bigelow, C. Fakhry, M. Windon, L.M. Rooper, P. Ha, B. Miles, C. Gourin, R. Mandal, W. Mydlarz, N. London, P.S. Vosler, S. Yavvari, T. Troy, T. Waterboer, D.W. Eisele, G. D'Souza, Oral Oncol. 121 (2021) 105461.
[50] R. Akyu Takei, K. Tomihara, M. Yamazaki, R. Moniruzzaman, W. Heshiki, K. Sekido, H. Tachinami, K. Sakurai, A. Yonesi, S. Imaue, K. Fujiwara, M. Noguchi, Oral Surg Oral Med Oral Pathol Oral Radiol 132 (2021) 549–565.
[51] S.T. Kim, S.Y. Kim, S.J. Klempner, J. Yoon, N. Kim, S. Ahn, H. Bang, K.M. Kim, W. Park, S.H. Park, J.O. Park, Y.S. Park, H.Y. Lim, S.H. Lee, K. Park, W.K. Kang, J. Lee, Ann. Oncol. 28 (2017) 547–554.
[52] R. Loewith, E. Jacinto, S. Wullschleger, A. Lorberg, J.L. Crespo, D. Bonenfant, W. Oppliger, P. Jenoe, M.N. Hall, Mol Cell 10 (2002) 457–468.
[53] H. Yang, X. Jiang, B. Li, H.J. Yang, M. Miller, A. Yang, A. Dhar, N.P. Pavletich, Nature 552 (2017) 368–373.
[54] K.H. Schreiber, S.I. Arriola Apelo, D. Yu, J.A. Brinkman, M.C. Velarde, F.A. Syed, C. Y. Liao, E.L. Baar, K.A. Carbajal, D.S. Sherman, D. Ortiz, R. Brunauer, S.E. Yang, S. T. Tzannis, B.K. Kennedy, D.W. Lamming, Nat. Commun. 10 (2019) 3194.
[55] G.J. Hanna, A. Villa, S.P. Nandi, R. Shi, A. Oneill, M. Liu, C.T. Quinn, N.S. Treister, H.Y. Sroussi, P. Vacharotayangul, L.A. Goguen, D.J. Annino, E.M. Rettig, V.Y. Jo, K.S. Wong, P. Lizotte, C.P. Paweletz, R. Uppaluri, R.I. Haddad, E.E.W. Cohen, L. B. Alexandrov, W.N. William, S.M. Lippman, S.-b. Woo, JAMA Oncol. 10 (2024).